Neutron star properties in a chiral SU(3) model

M. Hanauske, D. Zschiesche, S. Pal, S. Schramm, H. Stöcker, W. Greiner
Institut für Theoretische Physik, J.W. Goethe-Universität, D-60054 Frankfurt am Main, Germany

Abstract

We investigate various properties of neutron star matter within an effective chiral $SU(3)_L \times SU(3)_R$ model. The predictions of this model are compared with a Walecka-type model. It is demonstrated that the importance of hyperon degrees are strongly depending on the interaction used, even if the equation of state near saturation density is nearly the same in both models. While the Walecka-type model predicts a strange star core with strangeness fraction $f_S \approx 4/3$, the chiral model allows only for $f_S \approx 1/3$ and predicts that Σ^0, Σ^+ and Ξ^0 will not exist in star, in contrast to the Walecka-type model.

PACS: 26.60+c, 21.65+f, 24.10Jv

The internal constitution and properties of neutron stars chiefly depend on the nature of strong interactions. The accepted underlying theory of strong interactions, QCD, is however not solvable in the nonperturbative regime. So far numerical solutions of QCD on a finite space-time lattice are unable to describe finite nuclei or infinite nuclear matter [1]. As an alternative approach several effective models of hadronic interactions have been proposed [2–4]. Especially the Walecka model (QHD) and its nonlinear extensions have been quite successful and widely used for the description of hadronic matter and finite nuclei. These models are relativistic quantum field theories of baryons and mesons, but they do not consider essential features of QCD, like approximate $SU(3)_R \times SU(3)_L$ chiral symmetry or broken scale invariance. The Nambu–Jona-Lasinio (NJL) model [5,6] is an effective theory which has these features of QCD implemented but it lacks confinement and thereby fails to describe finite nuclei and nuclear matter. The chiral SU(3) models, for example the linear SU(3)-σ model [7] have been quite successful in modeling meson-meson interactions. The $K - N$ scattering data has been well reproduced using the chiral effective SU(3) Lagrangian [8,9]. However, all these chiral models lack the feature of including the nucleon-nucleon interaction on the same chiral SU(3) basis and therefore do not provide a consistent extrapolation to moderate and high densities relevant to the interior of a neutron star.

This has lead us to construct a QCD-motivated chiral $SU(3)_L \times SU(3)_R$ model as an effective theory of strong interactions, which implements the main features of QCD. The model has been found to describe reasonably well, the hadronic masses of the various SU(3) multiplets, finite nuclei, hypernuclei and excited nuclear matter [10,11]. The basic assumptions in the present chiral model are: (i) The Lagrangian is constructed with respect to the nonlinear realization of chiral $SU(3)_L \times SU(3)_R$ symmetry; (ii) The masses of the heavy baryons and mesons are generated by spontaneous symmetry breaking; (iii) The masses of the pseudoscalar mesons are generated by explicit symmetry breaking, since they are the Goldstone bosons of the model; (iv) A QCD-motivated field χ enters, which describes the gluon condensate (dilaton field) [12]; (v) Baryons and mesons are grouped according to their quark structure.

In this letter we investigate the composition and structure of neutron star matter with hyperons in this chirally invariant model. The total Lagrangian of the chiral $SU(3)_L \times SU(3)_R$ model for neutron star matter can be written in the mean-field approximation as (for details see Ref. [11])

$$\mathcal{L} = \mathcal{L}_{\rm kin} + \mathcal{L}_{\rm BM} + \mathcal{L}_{\rm BV} + \mathcal{L}_{\rm vec} + \mathcal{L}_0 + \mathcal{L}_{\rm SB} + \mathcal{L}_{\rm lep} \ , \tag{1}$$

where

$$\begin{aligned}
\mathcal{L}_{\rm BM} + \mathcal{L}_{\rm BV} &= -\sum_i \overline{\psi}_i \left[m_i^* + g_{i\omega}\gamma_0\omega^0 + g_{i\phi}\gamma_0\phi^0 + g_{N\rho}\gamma_0\tau_3\rho_0 \right] \psi_i \ , \\
\mathcal{L}_{\rm vec} &= \frac{1}{2} m_\omega^2 \frac{\chi^2}{\chi_0^2}\omega^2 + \frac{1}{2} m_\phi^2 \frac{\chi^2}{\chi_0^2}\phi^2 + \frac{1}{2}\frac{\chi^2}{\chi_0^2} m_\rho^2 \rho^2 + g_4^4(\omega^4 + 2\phi^4 + 6\omega^2\rho^2 + \rho^4) \ , \\
\mathcal{L}_0 &= -\frac{1}{2} k_0 \chi^2 (\sigma^2 + \zeta^2) + k_1(\sigma^2+\zeta^2)^2 + k_2(\frac{\sigma^4}{2} + \zeta^4) + k_3\chi\sigma^2\zeta \\
&\quad -k_4\chi^4 - \frac{1}{4}\chi^4 \ln\frac{\chi^4}{\chi_0^4} + \frac{\delta}{3}\ln\frac{\sigma^2\zeta}{\sigma_0^2\zeta_0} \ ,
\end{aligned}$$

$$
\begin{aligned}
\mathcal{L}_{\rm SB} &= -\left(\frac{\chi}{\chi_0}\right)^2\left[m_\pi^2 f_\pi \sigma + (\sqrt{2} m_K^2 f_K - \frac{1}{\sqrt{2}} m_\pi^2 f_\pi)\zeta\right] , \\
\mathcal{L}_{\rm lep} &= \sum_{l=e,\mu} \overline{\psi}_l [i\gamma_\mu \partial^\mu - m_l]\psi_l \ . \qquad (2)
\end{aligned}
$$

Here $\mathcal{L}_{\rm kin}$ is the kinetic energy term of the baryons and the scalar (σ, ζ) and vector (ω, ϕ, ρ) mesons. The interaction Lagrangian of the different baryons with the various spin-0 and spin-1 mesons are $\mathcal{L}_{\rm BM}$ and $\mathcal{L}_{\rm BV}$, respectively. The sum over i extends over all the charge states of the baryon octet $(p, n, \Lambda, \Sigma^-, \Sigma^0, \Sigma^+, \Xi^-, \Xi^0)$. $\mathcal{L}_{\rm vec}$ generates the masses of the spin-1 mesons through the interactions with spin-0 mesons, and $\mathcal{L}_0$ gives the meson-meson interaction term which induce the spontaneous breaking of chiral symmetry. A salient feature of the model, the dilaton field χ, which can be identified with the gluon condensate, is included. It accounts for the broken scale invariance of QCD at tree level through the logarithmic potential. $\mathcal{L}_{\rm SB}$ introduces an explicit symmetry breaking of the $\mathrm{U}(1)_A$, the $\mathrm{SU}(3)_V$, and the chiral symmetry. The last term $\mathcal{L}_{\rm lep}$ represents the free lepton Lagrangian. The effective masses of the baryons in the nonlinear realization of chiral symmetry are given by [11]

$$
\begin{aligned}
m_N^* &= m_0 - \frac{1}{3} g_{O8}^S (4\alpha_{OS} - 1)(\sqrt{2}\zeta - \sigma) \\
m_\Lambda^* &= m_0 - \frac{2}{3} g_{O8}^S (\alpha_{OS} - 1)(\sqrt{2}\zeta - \sigma) \\
m_\Sigma^* &= m_0 + \frac{2}{3} g_{O8}^S (\alpha_{OS} - 1)(\sqrt{2}\zeta - \sigma) \\
m_\Xi^* &= m_0 + \frac{1}{3} g_{O8}^S (2\alpha_{OS} + 1)(\sqrt{2}\zeta - \sigma) \ , \qquad (3)
\end{aligned}
$$

with $m_0 = g_{O1}^S(\sqrt{2}\sigma + \zeta)/\sqrt{3}$, in the usual notation [11]. The parameters g_{O1}^S, g_{O8}^S and α_{OS} are used to fit the vacuum baryon masses to their experimental values. The thermodynamic potential of the grand canonical ensemble per unit volume at zero temperature for the neutron star matter can be written as

$$
\Omega/V = -\mathcal{L}_{\rm vec} - \mathcal{L}_0 - \mathcal{L}_{\rm SB} - \mathcal{V}_{\rm vac} - \sum_i \frac{\gamma_i}{(2\pi)^3}\int d^3k \, [E_i^*(k) - \mu_i^*] - \frac{1}{3}\sum_l \frac{1}{\pi^2}\int \frac{dk\, k^4}{\sqrt{k^2 + m_l^2}} . \qquad (4)
$$

In Eq. (4) the vacuum energy $\mathcal{V}_{\rm vac}$ has been subtracted. For a given baryon species i, the single particle energy and chemical potential are respectively,

$$
\begin{aligned}
E_i^*(k) &= \sqrt{k_i^2 + m_i^{*2}} \ , \\
\mu_i &= b_i \mu_n - q_i \mu_e = \mu_i^* + g_{i\omega}\omega_0 + g_{i\phi}\phi_0 + g_{i\rho} I_{3i}\rho_0 \ , \qquad (5)
\end{aligned}
$$

with $\mu_i^* \equiv E_i^*(k = k_{F_i})$; b_i and q_i are the baryon number and charge of the ith species. The energy density and pressure follows from the Gibbs-Duhem relation, $\varepsilon = \Omega/V + \sum_{k=i,l} \mu_k \rho_k$ and $P = -\Omega/V$. At a given baryon density ρ_B, the field equations as obtained by extremizing Ω/V are solved self-consistently in conjunction with the charge neutrality and β-equilibrium conditions.

The parameters of the chirally invariant potential, k_0 and k_2, are used to ensure an extremum in the vacuum, while k_3 is constrained by the η' mass, and k_1 is varied to give $m_\sigma = 500$ MeV. The vacuum expectation value of the fields σ and ζ are constrained by the pion and kaon decay constants, $\sigma_0 = f_\pi$ and $\zeta_0 = -(2f_K - f_\pi)/\sqrt{2}$. The parameters $g_{N\omega}$ and χ_0 are used to fit the binding energy of nuclear matter $B/A = \varepsilon/\rho_B - m_N = -16$ MeV at the saturation density $\rho_0 = 0.15$ fm^{-3}. In the present calculation we have employed the parameter set C1 of Ref. [11]. The predicted values of effective nucleon mass, incompressibility, and symmetry energy at the saturation density are $m_N^*/m_N = 0.61$, $K = 276$ MeV, and $a_{\rm sym} = 40.4$ MeV. The remaining couplings to the strange baryons are then determined by the additive quark model constraints:

$$g_{\Lambda\omega} = g_{\Sigma\omega} = 2g_{\Xi\omega} = \frac{2}{3}g_{N\omega} = 2g_{O8}^V; \qquad g_{\Lambda\phi} = g_{\Sigma\phi} = \frac{g_{\Xi\phi}}{2} = \frac{\sqrt{2}}{3}g_{N\omega} \ . \tag{6}$$

Figure 1 shows the energy per baryon as a function of baryonic density ρ_B for varying neutron-proton asymmetries, $\delta = (\rho_n - \rho_p)/\rho_B$, calculated in the chiral model. The curve $\delta = 0$ describes infinite symmetric nuclear matter with a minimum at ρ_0. With increasing asymmetry, ($\delta > 0$) the binding energy decreases and the saturation density is shifted to lower values. The binding in nuclear matter for small values of δ stems from the isospin symmetric nuclear forces. At asymmetries $\delta \geq 0.84$ (i.e. a neutron to proton ratio > 11), the system starts to become unbound even at the low density regimes. The stiffest equation of state (EOS) is obtained for pure neutron matter with $\delta = 1$. Due to the β-equilibrium conditions, the EOS for neutron star matter (labeled NS) composed of neutrons, protons and electrons (*npe*) is softer as compared to pure neutron matter. The gravitational attraction provides the necessary binding of neutron stars. The present results from the chiral model corroborate those obtained in Walecka-like models [13,14] and in the relativistic Brueckner-Hartree-Fock calculations [15].

Let us now discuss the inclusion of hyperons. With the choice of the parameter set discussed above, the chiral model is found to produce unrealistically large hyperon potential depths in nuclear matter in comparison to the experimental values of $U_{\Lambda,\Xi}^N \approx -28$ MeV for the Λ and Ξ particle. Parameter sets that reproduce reasonable values of $U_{\Lambda,\Xi}^N$ are, however, found to yield unsatisfactory nuclear properties [11]. Fortunately, explicit symmetry breaking can be introduced in the nonlinear realization without affecting, e.g., the partially conserved axial-vector currents relations. This allows for the inclusion of additional terms for the hyperon-scalar meson coupling [11]:

$$\mathcal{L}_{\rm hyp} = m_3 {\rm Tr}\left(\overline{\psi}\psi + \overline{\psi}\left[\psi, S\right]\right) {\rm Tr}\left(X - X_0\right) \ , \tag{7}$$

where X represents a scalar and $S_b^a = -[\sqrt{3}(\lambda_8)_b^a - \delta_b^a]/3$ with λ's are the usual Gell-Mann matrices. In the mean field approximation this leads to the following additional mass term

$$\widetilde{m}_i^* = m_i^* + a\, m_3 \left[\sqrt{2}(\delta - \delta_0) + (\zeta - \zeta_0)\right], \tag{8}$$

where m_i^* is given by Eq. (3). With $a = n_s$, where n_s is the number of strange quarks in the baryon, and, with the parameter m_3 adjusted to $U_\Lambda^N = -28$ MeV, the other hyperon potentials obtained are $U_\Sigma^N = +3.2$ MeV, and $U_\Xi^N \sim +30$ MeV. Since the potential of Ξ in ground state nuclear matter is still not satisfactory, we have used $a = 1$ as an alternative

parametrization. For $U_\Lambda^N = -28$ MeV, one obtains now $U_\Sigma^N = +3.2$ MeV, and $U_\Xi^N = -42$ MeV. We are well aware that our choice of the parametrization of the hyperon potentials is not unique; the examination of different ways of generating the experimentally favored values for U_Σ^N and U_Ξ^N is in progress and will be reported in a different context. Hereafter we have employed $a = 1$ in our calculations.

Let us compare the results obtained in the chiral model with that of a Walecka-type model. The latter model employed here has a cubic and quartic self-interaction for the σ field, $U(\sigma) = g_2\sigma^3/3 + g_3\sigma^4/4$, introduced to get correct nuclear matter compressibility [3], and a quartic self-interaction for the vector field ω, $\mathcal{L}_v = g_4(\omega^\mu\omega_\mu)^2$. This modification leads to a reasonable reproduction of the Dirac-Brueckner calculation [16]. We have used the parameter set TM1 of Ref. [16] which gives a saturation density and binding energy of $\rho_0 = 0.145$ fm^{-3} and $B/A = -16.3$ MeV. It is to be noted that in the TM1 set, the values of $m_N^*/m_N = 0.63$, $K = 281$ MeV, and $a_{\rm sym} = 36.9$ MeV which primarily influence the bulk properties of neutron star matter are nearly identical to those in the chiral model. The hyperon couplings σ-Y are obtained from a depth of $U_Y^N = -28$ MeV, while the ω-Y couplings are obtained from SU(6) symmetry relations (6). Two additional strange mesons, ζ and ϕ, are introduced which couple only to the hyperons. The ζ-Y couplings are fixed by the condition $U_\Xi^\Xi \approx 2U_\Lambda^\Lambda \approx -40$ MeV [17,18].

Figure 2 shows the particle fractions versus the baryonic density in β-equilibrated matter in the chiral model (top panel) and the Walecka-type model, TM1 (bottom panel). With increasing density, it is energetically favorable for nucleons at the top of the Fermi sea to convert into other baryons. Note that the sequence of appearance of the hyperon species is the same in both models. The first strange particle to appear is the Σ^-, since its somewhat higher mass (as compared to the Λ) is compensated by the electro-chemical potential in the chemical equilibrium condition (5). Because of its negative charge, charge neutrality can be achieved more economically which causes a drop in the lepton fraction. More massive and positively charged particles than these appear at higher densities. These are in fact generic features found in neutron star calculations with hyperons [13,14,19,20]. Because of the equilibrium condition (5), the threshold densities of the different hyperon species are, however, strongly dependent on the magnitude of the scalar and vector fields at a given density and their interactions with the baryons. The nucleon-nucleon interaction which determines the variation of neutron chemical potential with density also determines the threshold. The relatively smaller attractive scalar fields and thereby larger effective mass of all the baryons cause a significant shift of the density at which the hyperons $(\Sigma^0, \Sigma^+, \Xi^0)$ appear in the chiral model calculation. This enhances the saturation values of both the neutron and proton fractions (at a level of $\sim 30\%$) in the chiral model. Consequently, the cores of massive stars in the TM1 model (and also in other Walecka-type models [18]) are in general predicted to be very ($> 50\%$) hyperon-rich. The chiral model, on the other hand, predicts neutron stars with considerable smaller hyperon fractions in the core.

The composition of the star is crucial for neutrino and antineutrino emission which can be responsible for the rapid cooling of neutron stars via the URCA process. It was demonstrated [21] that for a *npe* system rapid cooling by nucleon direct URCA process is allowed when the momentum conservation condition $k_{F_p} + k_{F_e} \geq k_{F_n}$, corresponding to a proton fraction $Y_p \geq 0.11$, is satisfied. The magnitude of Y_p at a given ρ_B, in turn, is determined mainly by the symmetry energy, which is nearly identical in the two models. Therefore, in both

models this condition is satisfied at densities $\rho_B \gtrsim 2.2\rho_0$ thus, rapid cooling by direct URCA process can occur.

The most profound implication of the constitution of neutron star matter on its bulk properties are manifested in the equation of state (EOS). The pressure P versus the energy density ε is displayed in Fig. 3 for neutron star matter in the chiral (thick lines) and TM1 (thin lines) model. For *npe* stars (solid lines), although the incompressibility K and the effective nucleon mass m_N^* at the normal nuclear matter density are similar in the two models, the EOS at large densities is found to be considerably softer for the chiral model as compared to the EOS for TM1. In the latter model, the m_N^* rapidly decreases with density, consequently the EOS passes quickly to one that is dominated by the repulsive vector mesons (ω and ρ) leading to a stiffer EOS. This has a strong bearing on the mass and radius of such stars discussed below. The structure of static neutron stars can be determined by solving the Tolman-Oppenheimer-Volkoff equations [22]. We use the results of Baym, Pethick and Sutherland [23] to describe the crust consisting of leptons and nuclei at the low-density ($\rho_B < 0.001$ fm^{-3}) EOS. For the mid-density regime ($0.001 < \rho_B < 0.08$ fm^{-3}) the results of Negele and Vautherin [24] are employed. Above this density, the EOS for the relativistic models have been adopted. The masses M of the nonrotating neutron star sequence is shown in Fig. 4 as a function of central energy density ε_c in the two models. The corresponding mass-radius relationship is presented in Fig. 5. It is observed that the stiffer EOS for a *npe* star in the TM1 model can support a larger maximum mass of $M_{\rm max} = 2.16 M_\odot$ with a corresponding radius of $R_{M_{\rm max}} = 11.98$ km at a central baryonic density of $\rho_c = 6.08\rho_0$. The corresponding values obtained in the chiral model are $M_{\rm max} = 1.84 M_\odot$, $R_{M_{\rm max}} = 11.10$ km, and $\rho_c = 6.98\rho_0$. The large difference in the $M_{\rm max}$ values obtained in the two models, with nearly identical K and m_N^* values at ρ_0, clearly demonstrates that measurements of maximum masses of neutron (*npe*) stars at high densities cannot be used to constrain the incompressibility and the effective nucleon mass around the nuclear matter densities. Constraints on K and m_N^* from radius measurements of massive stars will be even more uncertain, since about 40% of these stars' radius originates from the low density EOS. In fact, no precise radius measurements currently exist.

When the hyperon degrees of freedom are included, the EOS (represented by dash-dotted lines in Fig. 3) for both the models are appreciably softer as compared to *npe* stars. This is caused by the opening of the hyperon degrees of freedom which relieves some of the Fermi pressure of the nucleons. Also the decrease of the pressure exerted by the leptons (they are replaced by negatively charged hyperons to maintain charge neutrality) contributes to softening of the EOS. Since the threshold density for the appearance of the hyperons, especially $(\Sigma^0, \Sigma^+, \Xi^0)$ (see Fig. 2), are smaller in TM1 model, these stars contain more baryon species. This leads to an enhanced softening as compared to that in the chiral model. In fact, both models with hyperons predict quite similar values of pressure at moderate and high densities; the structures observed in the EOS (Fig. 3) correspond to the population of different hyperon species. These should reflect both in the masses and radii of the stars. The maximum masses and corresponding radii of stars with hyperons in the two models are almost identical with $M_{\rm max} = 1.52 M_\odot$, $R_{M_{\rm max}} = 11.64$ km, and $\rho_c = 5.92\rho_0$ in the chiral model, while in the TM1 model, $M_{\rm max} = 1.55 M_\odot$, $R_{M_{\rm max}} = 12.14$ km, and $\rho_c = 5.97\rho_0$. The magnitude of the central densities indicates that the hyperons $(\Sigma^0, \Sigma^+, \Xi^0)$ are entirely precluded in stars for the chiral model whereas all hyperon species appear with

comparable abundances in the TM1 model for the maximum-mass star. The strangeness fraction, $f_S = \sum_i |S_i|\rho_i/\rho_B$, are vastly different at the center of the maximum-mass stars: 0.33 vs. 0.75 in the chiral and in the TM1 model, respectively. Thus, models with similar nuclear matter incompressibilities and effective nucleon masses, leading to similar maximum star masses and corresponding similar radii can however have a widely different baryonic constitution!

For progressively smaller central densities, the masses of the stars with hyperons are larger in the TM1 model (see Fig. 4), although the pressure at a given density is smaller than in the chiral model. This is because the masses of stars are determined by the overall EOS, and the TM1 model possess a distinctively stiffer EOS at moderate densities (see Fig. 3). The radii of these small mass hyperon-rich stars are quite distinct in these two models (see Fig. 5), because the radius of the stars depend most sensitively on the low density behavior of the EOS. In both models, stars of mass $1.44 M_\odot$ (corresponding to the lower limit imposed by the larger mass of the binary pulsar PSR 1913+16 [25]) also contain many hyperon species with sizeable concentration.

In conclusion, we have investigated the composition and structure of neutron star matter in a novel chiral SU(3) model, and compared its predictions with that of a Walecka-type model based on different underlying assumptions. The two models with nearly identical values of effective nucleon mass, incompressibility, and symmetry energy at the normal nuclear density yield widely different maximum neutron star masses and radii. When the hyperon degrees of freedom are included, the maximum masses and the corresponding radii in the two models are found to be rather similar. However, softness of the nucleonic contribution in the chiral model precludes the hyperons $\Sigma^0, \Sigma^+, \Xi^0$ leading to much smaller hyperon abundances in these stars.

ACKNOWLEDGMENTS

The authors are thankful to N. Glendenning, F. Weber and J. Schaffner-Bielich for helpful discussions. This work was funded in part by the Gesellschaft für Schwerionenforschung (GSI), the DFG and the Hessische Landesgraduiertenförderung. S.P. acknowledges support from the Alexander von Humboldt Foundation.

REFERENCES

[1] J.D. Walecka, *Theoretical Nuclear and Subnuclear Physics* (Oxford University Press, New York, 1995).

[2] B.D. Serot and J.D. Walecka, Adv. Nucl. Phys. 16 (1986) 1.

[3] J. Boguta and A.R. Bodmer, Nucl. Phys. A 292 (1977) 413;
J. Boguta and H. Stöcker, Phys. Lett. B120 (1983) 289.

[4] R.J. Furnstahl, C.E. Price, and G.E. Walker, Phys. Rev. C 36 (1987) 2590.

[5] Y. Nambu and G. Jona-Lasinio, Phys. Rev. 122 (1961) 345; 124 (1961) 246.

[6] P. Rehberg, S. Klevansky, and J. Hüfner, Phys. Rev. C 53 (1996) 410.

[7] N.A. Törnqvist, hep-ph/9711483.

[8] T. Waas and W. Weise, Nucl. Phys. A 625 (1997) 287.

[9] A. Ramos and E. Oset, Nucl. Phys. A 635 (1998) 99.

[10] P. Papazoglou, S. Schramm, J. Schaffner-Bielich, H. Stöcker, and W. Greiner, Phys. Rev. C 57 (1998) 2576.

[11] P. Papazoglou, D. Zschiesche, S. Schramm, J. Schaffner-Bielich, H. Stöcker, and W. Greiner, Phys. Rev. C 59 (1999) 411.

[12] J. Schechter, Phys. Rev D 21 (1980) 3393.

[13] N.K. Glendenning, *Compact Stars* (Springer, New York, 1997).

[14] F. Weber, *Pulsars as Astrophysical Laboratories for Nuclear and Particle Physics* (IoP, Bristol, 1999).

[15] L. Engvik, M. Hjorth-Jensen, E. Osnes, G. Bao, and E. Østgaard, Phys. Rev. Lett. 73 (1994) 2650.

[16] Y. Sugahara and H. Toki, Nucl. Phys. A 579 (1994) 557.

[17] J. Schaffner, C.B. Dover, A. Gal, D.J. Millener, C. Greiner, and H. Stöcker, Ann. Phys. (N.Y.) 235 (1994) 35.

[18] J. Schaffner and I. Mishustin, Phys. Rev. C 43 (1996) 1416.

[19] M. Prakash, I. Bombaci, M. Prakash, P.J. Ellis, J.M. Lattimer, and R. Knorren, Phys. Rep. 280 (1997) 1.

[20] S. Pal, M. Hanauske, I. Zakout, H. Stöcker, and W. Greiner, Phys. Rev. C 60 (1999) 015802.

[21] J.M. Lattimer, C.J. Pethick, M. Prakash, and P. Haensel, Phys. Rev. Lett. 66 (1991) 2701.

[22] R.C. Tolman, Phys. Rev. 55 (1939) 364;
J.R. Oppenheimer and G.M. Volkoff, Phys. Rev. 55 (1939) 374.

[23] G. Baym, C. Pethick, and P. Sutherland, Astrophys. J. 170 (1971) 299.

[24] J. Negele and D. Vautherin, Nucl. Phys. A 207 (1973) 298.

[25] J.M. Weisberg and J.H. Taylor, Phys. Rev. Lett. 52 (1984) 1348.

FIGURES
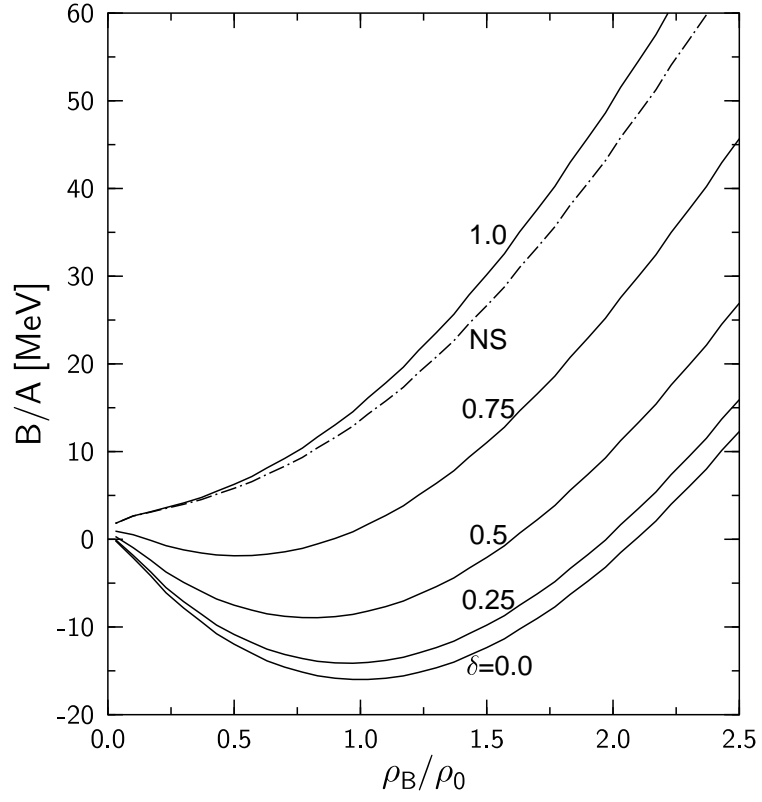
FIG. 1. The binding energy per nucleon B/A versus the baryonic density ρ_B/ρ_0 for different values of neutron-proton asymmetries $\delta = (\rho_n - \rho_p)/\rho_B$ in the chiral model. The normal nuclear matter density is $\rho_0 = 0.15$ fm^{-3}. The curve labeled NS describes a neutron star matter consisting of nucleons and electrons.
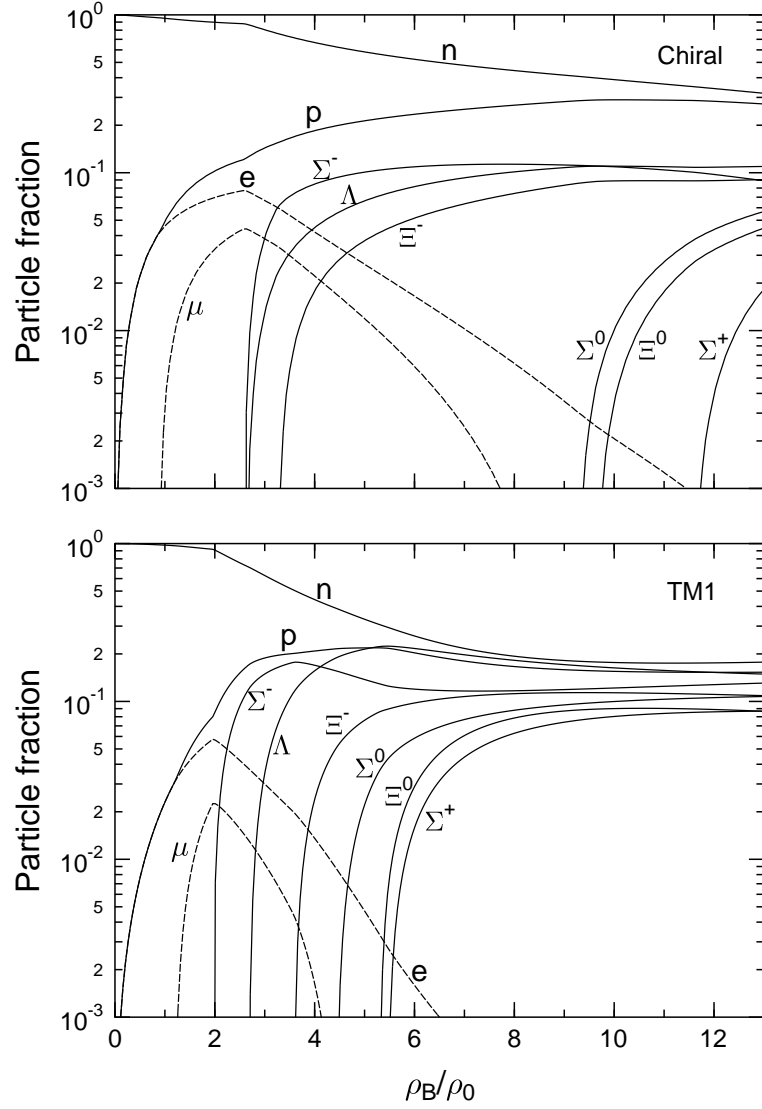
FIG. 2. The composition of neutron star matter with hyperons in the chiral (top panel) and in the TM1 (bottom panel) model. The normal nuclear matter density is $\rho_0 = 0.15$ and 0.145 fm^{-3} in the chiral and TM1 model.
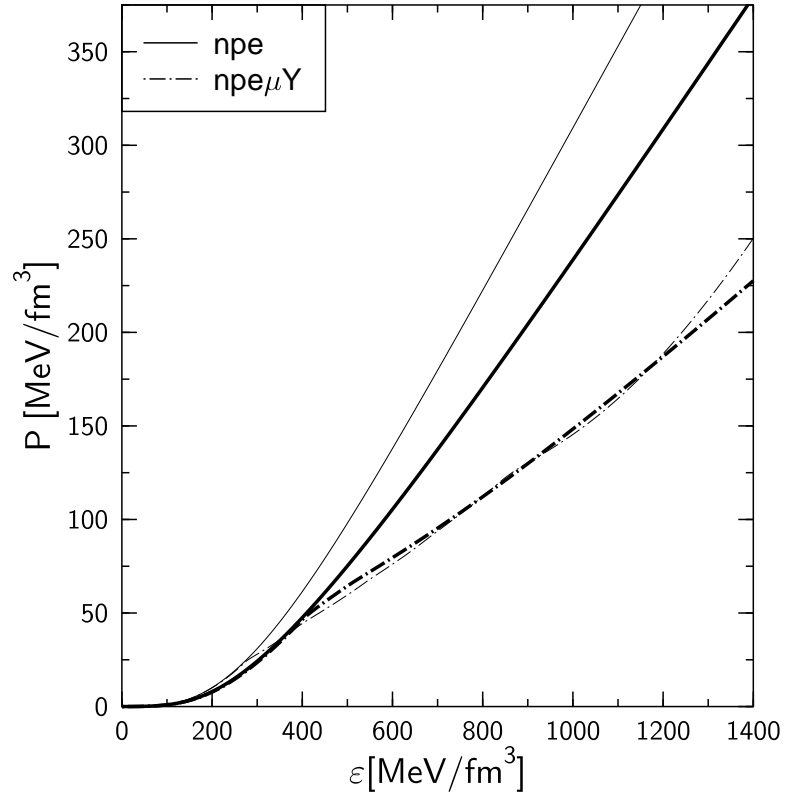
FIG. 3. The equation of state, i.e. the pressure P, versus the energy density ε. The results are for *npe* stars (solid lines), and for stars with further inclusion of hyperons and muons (dash-dotted lines). The calculations are in the chiral model (thick lines) and in the TM1 model (thin lines).
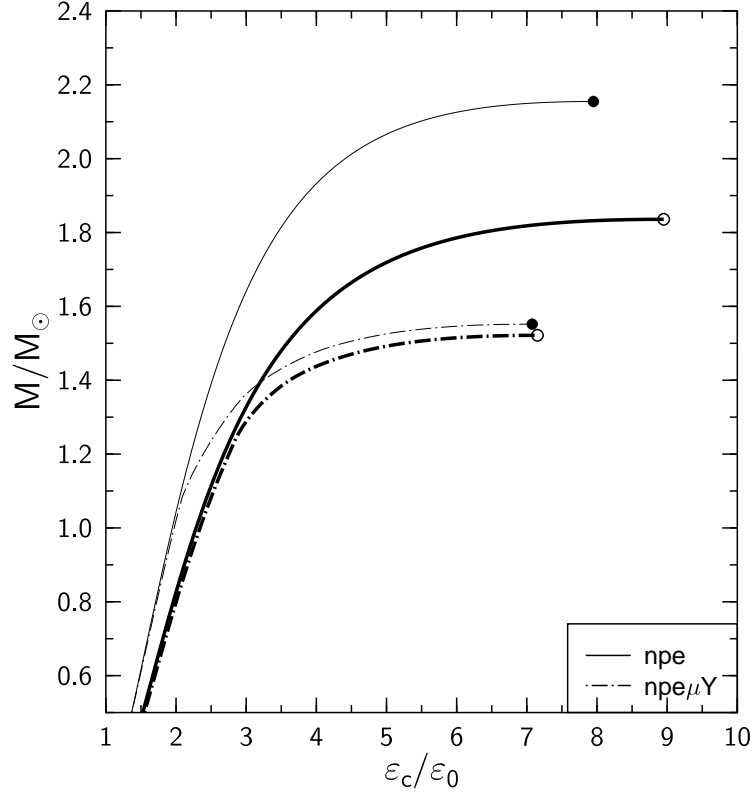
FIG. 4. The mass as a function of central energy density $\varepsilon_c/\varepsilon_0$ for *npe* stars and for stars with further inclusion of hyperons and muons in the chiral and TM1 models. The chiral model results are represented by thick lines, and the TM1 results are given by the thin lines. The circles correspond to the respective maximum masses. The central energy density at normal nuclear matter value is $\varepsilon_0 = 142.9$ and 137.0 MeV/fm^3 in the chiral and in the TM1 model, respectively.
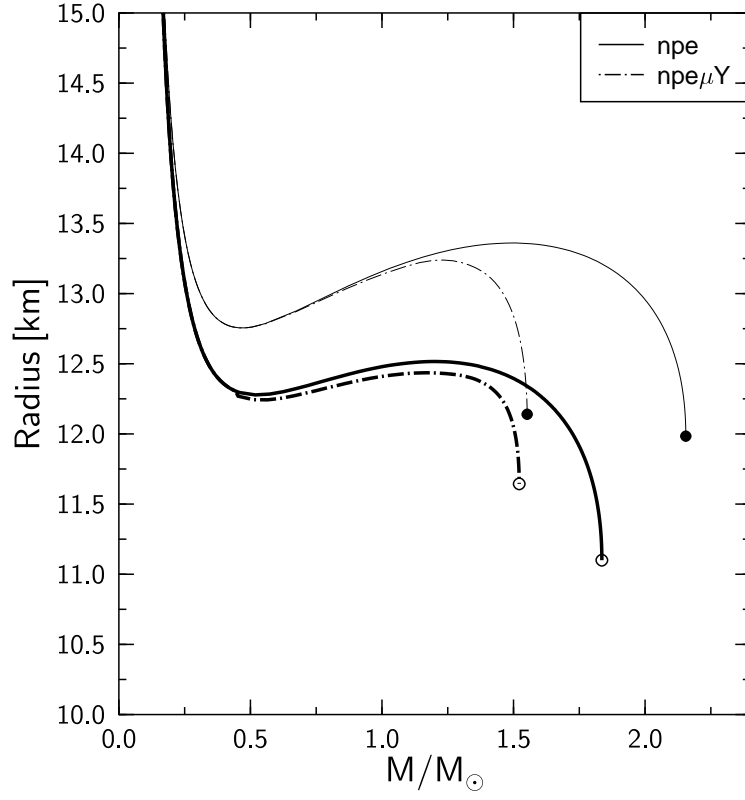
FIG. 5. The mass as a function of radius for neutron stars consisting of *npe* and for stars with further inclusion of hyperons and muons in the chiral and TM1 model. The symbols have the same meaning as in Fig. 4.